Available online at www.sciencedirect.com
SCIENCE DIRECT®
International Journal of Heat and Mass Transfer 47 (2004) 5115–5128
International Journal of HEAT and MASS TRANSFER
www.elsevier.com/locate/ijhmt

Marangoni heat transfer in subcooled nucleate pool boiling

Sanja Petrovic, Tony Robinson, Ross L. Judd *

Department of Mechanical Engineering, McMaster University, Hamilton, Ont., Canada L8S 4L7

Received 5 December 2003; received in revised form 20 May 2004
Available online 18 August 2004

Abstract

The liquid motion induced by surface tension variation, termed the Marangoni effect, and its contribution to boiling heat transfer has been an issue of much controversy. Boiling heat transfer theory, although acknowledging its existence, considers its contribution to heat transfer to be insignificant in comparison with buoyancy induced convection. However, recent microgravity experiments have shown that although the boiling mechanism in a reduced gravity environment is different, the corresponding heat transfer rates are similar to those obtained under normal gravity conditions, raising questions about the validity of the assumption. An experimental investigation was performed in which distilled water was gradually heated to boiling conditions on a copper heater surface at four different levels of subcooling. Photographic investigation of the bubbles appearing on the surface was carried out in support of the measurements. The results obtained indicate that Marangoni convection associated with the bubbles formed by the air dissolved in the water which emerged from solution when the water was heated sufficiently, significantly influenced the heat transfer rate in subcooled nucleate pool boiling. A heat transfer model was developed in order to explain the phenomena observed.

1. Introduction

Due to its high efficiency, nucleate boiling, with its wide range of possible applications, has been studied extensively over the past decades. Nucleate boiling is associated with a change in phase from liquid to vapour at a solid–liquid interface, which is characterized by the formation of vapour bubbles that nucleate, grow and subsequently detach from specific locations on the surface called nucleation sites, that occurs when the surface temperature exceeds the liquid saturation temperature at the corresponding liquid pressure. One of the main characteristics of the nucleate boiling process is the very high heat transfer rates associated with the phenomenon, making the application especially valuable when limited space is available to accomplish large energy transfer.

Despite the great technical importance and the extensive experimental and theoretical studies that have been performed, boiling heat transfer is still not well understood, primarily because of its complexity. Because of the latent heat of evaporation released by the virtue of the phase change, the theories developed emphasized the influence of the buoyancy force which arises from the density difference between the liquid and vapour phase in the presence of a gravitational field and causes the vapour bubbles to detach from the heated surface. The thermocapillary or Marangoni effect, induced by

* Corresponding author. Tel.: +1 905 525 9140; fax: +1 905 572 7944.
E-mail address: juddr@mcmaster.ca (R.L. Judd).

0017-9310/$ - see front matter © 2004 Elsevier Ltd. All rights reserved.
doi:10.1016/j.ijheatmasstransfer.2004.05.031

Nomenclature

A	area (m^2)
C	specific heat (J/kg K)
f	frequency of bubble emission (Hz)
g	gravitational acceleration (m/s^2)
H	Henry's law constant (atmospheres of air pressure/(moles air/mole water))
h	heat transfer coefficient (W/m^2K)
k	thermal conductivity (W/m K)
L	characteristic length (m)
N	number of bubbles
p	pressure (Pa, atmos)
q''	heat flux (W/m^2)
R, r	radius (m)
T	temperature (°C)
t_g	growth time (s)
t_w	waiting time (s)
V	velocity (m/s)
VP	vapour pressure of water (Pa, atmos)
x	mole fraction
z	distance from the surface (m)

Greek symbols

α	thermal diffusivity (m^2/s)
β	volumetric thermal expansion coefficient (1/°C)
δ	superheated layer thickness (m)
μ	dynamic viscosity (Ns/m^2)
ν	kinematic viscosity (m^2/s)
θ	temperature difference (°C)
ρ	density (kg/m^3)
$\sum$	sum
σ	surface tension (N/m)

Dimensional numbers

Gr	Grashof number, $\frac{g\beta(T_w - T_\infty)L^3}{\nu^2}$
Ma	Marangoni number, $\frac{\frac{d\sigma}{dT}\frac{dT}{dz}R_b^2}{\mu\alpha}$
Nu	Nusselt number, hL/k
Pr	Prandtl number, ν/α
Ra	Rayleigh number, $\frac{g\beta(T_w - T_\infty)L^3}{\nu\alpha}$

Subscripts

atmos	atmospheric
b	bottom/bubble
bt	bubbles total
c	cavity
cond	conduction
i	ith bubble
L	characteristic length
l	liquid
m	Marangoni/middle
nb	nucleate boiling
nc	natural convection
sat	saturation
sub	subcooled
sup	superheat
t	top/total
v	vapour
w	heater wall
∞	bulk liquid

the surface tension variation at the vapour–liquid interface, was assumed to be negligible and its contribution to heat transfer was not taken into consideration. However, experiments performed in a microgravity environment by Straub [1] showed that the boiling process was attainable even when buoyancy was greatly reduced and furthermore, that the heat transfer rates obtained were similar to those obtained under terrestrial conditions. These surprising results led to a series of investigations in order to determine the mechanism responsible for the behaviour observed. Contrary to what was previously assumed, it is now believed that the Marangoni effect is significant and its contribution to boiling heat transfer must not be overlooked. This study is an attempt to investigate convection heat transfer due to the Marangoni effect in subcooled nucleate pool boiling water at atmospheric pressure. The experiments were performed at four different levels of subcooling 40, 50, 60 and 70 °C and different levels of surface heat flux varying over a range up to 700 kW/m^2.

2. Literature review

2.1. Surface tension induced flow

The liquid motion due to the surface tension variation at a gas/liquid interface, referred to as the Marangoni effect, has been studied in the past by various researchers from different perspectives. Early works by Pearson [2], Scriven and Sternling [3] and Smith [4] dealt with the onset of cellular motion and the flow stability produced in terms of the dimensionless Marangoni number, representing the ratio between the surface tension and viscous forces, defined as

$$Ma = \frac{(d\sigma/dT)(dT/dz)}{\mu_l \alpha_l} d^2 \quad (1)$$

By employing linear stability analysis, these researchers argued the existence of a minimum, or critical, value of Marangoni number, Ma_c, above which the transition

from the buoyancy to the surface tension driven flow would occur.

The effect of temperature variation on a spherical free surface was examined first by Young et al. [5] who observed experimentally that the small air bubbles in a liquid sample could be held stationary or driven downwards by a sufficiently strong negative temperature gradient in the vertical direction. The phenomenon was attributed to the surface tension variation at the bubble surface due to the temperature field present.

That Marangoni flow might be of importance as a heat transfer mechanism in nucleate boiling was originally suggested by McGrew et al. [6] who questioned the explanation that high boiling heat transfer rates are attributed to intense vapour bubble agitation of the liquid boundary layer adjacent to the heating surface and bulk liquid entrainment by bubble detachment from the surface. A series of experiments was performed in which the liquid was heated from above and cooled from below, with slowly increasing heat flux. Observations of the flow profile around air bubbles placed on the heating surface and vapour bubbles produced during boiling conditions were enabled by small tracer particles suspended in the liquid. As a result of the identical flow patterns observed around air bubbles and vapour bubbles, McGrew concluded that Marangoni flow would occur around any bubble present in a region subjected to a temperature gradient and that the phenomenon observed served as a primary factor in the heat transfer mechanism in those situations where bubbles remained attached to the surface for relatively long periods of time.

2.2. Flow distribution around a bubble on a heated wall

Since liquids, in general, have a negative temperature coefficient of surface tension, the preferred set-up in the majority of experiments performed is that shown in Fig. 1. Heating the liquid from above ensures that buoyancy and surface tension forces act in opposite directions so that Marangoni flow cannot be overwhelmed by buoyancy driven flow. The studies performed all agreed on the general liquid flow profile around a spherical gas bubble attached to a heater surface. The difference in the temperature of the bubble at its base and at its top establishes the surface tension gradient which leads to a liquid flow in the direction of increasing surface tension. Although the resulting surface tension force is opposed by the shear stresses within both the gas and liquid phase, the shear stress in the liquid is much larger than that in the gas, leading to the conclusion that the shear forces on the gas side at the gas/liquid interface can be neglected.

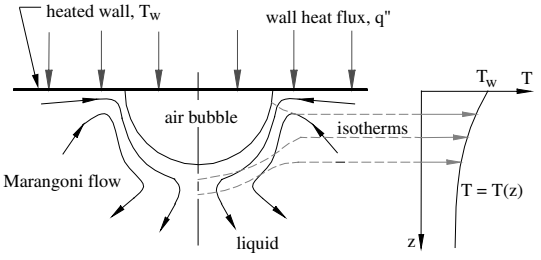

Fig. 1. Surface tension induced flow around an air bubble at a heated wall.

The first numerical study of the Marangoni effect around a hemispherical bubble placed on a solid wall subjected to constant heat flux was conducted by Larkin [7] who obtained time dependent numerical solutions for the flow and temperature fields, which were dependent upon the Prandtl number and the Marangoni number, for Prandtl numbers of 1 and 5 and Marangoni numbers ranging from 0 to 10^5. The liquid was observed to move toward the wall, then flow around the bubble surface and leave the bubble as a jet. The extent of the jet increased with increasing Marangoni number and decreased with increasing Prandtl number. Larkin reported that the flow built up quickly and then gradually declined with time but was unable continue the solution until steady-state was reached because of the enormous computer time required.

A theoretical estimate of surface tension induced flow on the thermal equilibrium of a vapour bubble located at a heated wall was investigated by Gaddis [8] for the range of Marangoni numbers between 0 and 125 and Biot numbers from 0 to 100. Gaddis concluded that the surface tension induced fluid flow reduced the temperature difference between the wall and the vapour inside the bubble and therefore resulted in a lower wall superheat needed for the incipience of nucleate boiling. The analysis performed by Kao and Kenning [9] extended the work of Larkin and Gaddis by examining the steady-state flow for a range of Marangoni numbers from 50 to 2.5×10^5 and Biot numbers from 0 to 5000. Their observations were in qualitative agreement with those previously reported by Larkin. They also showed that even a small amount of contaminants could produce considerable differences in liquid properties, resulting in the suppression of Marangoni flow.

The most comprehensive description of the Marangoni flow was given by Hupik and Raithby [10] who examined surface tension effects in water boiling on a downward facing heated surface. The water temperature in all experiments performed was below the saturation temperature. An air bubble placed on the wall resulted in a formation of a strong jet of fluid, moving downward along the centerline of the bubble. The surrounding cooler liquid was induced to flow toward the heater surface and the base of the bubble. At heat fluxes large enough to produce a large number of vapour bubbles, an

increased tendency of bubbles to coalesce was observed, resulting in the formation of a vapour blanket that covered a large portion of the surface. Vigorous Marangoni flow was observed at the periphery of the blanket, drawing the liquid over the heater surface and propelling it along the vapour interface.

An important observation was reported in the comprehensive work of Schwabe and Metzger [11] concerning the relative importance of the surface tension induced flow in liquid crystal growth with high Prandtl number. In their experiments, ethanol was placed in a rectangular cavity with a free upper surface. The temperature gradient in the bulk liquid was provided by means of two bulk heaters placed at diametrically opposite locations on the outer wall of the cavity. In order to vary the temperature difference across the free surface independently from that in the bulk liquid, two thin surface heaters were placed at the surface level above the corresponding bulk heaters from which they were thermally insulated. In this way, it was possible to vary the temperature gradient in the bulk liquid and across the surface independently and consequently to separate the influence of the buoyant and surface tension forces. The results obtained clearly showed the Marangoni flow produced and its increasing significance with increasing temperature gradient. The surface tension forces observed were always significant in the experiments performed and the authors recommended that surface tension effects should be given much more attention.

Wozniak et al. experimentally examined the effectiveness of particle–image–velocimetry for the visualisation of the flow induced by surface tension variation in both normal gravity, Wozniak, Wozniak and Rosgen [12] and reduced gravity, Wozniak, Wozniak and Bergelt [13]. Normal gravity experiments, performed again with an air bubble inserted in silicon oil under a heated wall facing downward, clearly identified the flow pattern which led to the conclusion that the technique employed could be used effectively for Marangoni flow investigations. The experiments performed in microgravity, where the surface tension variation was the only reason for the induced flow, showed that the influence of the flow produced penetrated much deeper into the bulk liquid and led to a jet-like liquid flow.

For higher Marangoni numbers, oscillatory Marangoni flow was observed and reported by various researchers [11,14–18].

2.3. Marangoni heat transfer

The first attempt to examine the relevance of Marangoni heat transfer was performed by Larkin in the course of his analytical study on Marangoni flow around a hemispherical bubble. By making a number of assumptions, Larkin analyzed the influence of the surface tension driven flow on the Nusselt number and concluded that the impact of the mechanism on heat transfer was an increase of only 30% in the rate of heat transfer at a very high Marangoni number of 10^5. Larkin concluded that before Marangoni convection became an important heat transfer mechanism, the Marangoni number had to exceed a value of 10^5. However, boiling experiments performed in microgravity led to the striking observation that the heat transfer coefficient in nucleate boiling was hardly influenced by the gravity level according to Straub et al. [19] for a wide range of fluid states and heat fluxes examined. The conclusion was in strong contradiction with the existing boiling theories which generally assumed that the heat transport mechanism was dominated by buoyancy forces due to the density difference between the liquid and vapour phase. Gravity was therefore seen as an important factor in all physical based or empirical correlations for pool boiling heat transfer. Microgravity experimental results raised questions about the mechanism responsible for high heat transfer rates obtained under reduced gravity conditions since buoyancy was suppressed in those cases and was no longer playing a role in the heat transfer process. Straub pointed out that among mechanisms neglected in the boiling heat transfer models was Marangoni convection which was caused by the surface tension variation and was therefore independent of gravity. From a series of experiments and numerical investigations, Straub demonstrated that, contrary to what was believed until then, surface tension induced flow was significant and that its contribution to heat transfer could not be neglected. Furthermore, an experimental investigation with an air bubble resting on a platinum wire heater submerged in methanol showed 100% increase in the heat transfer rates due to the Marangoni convection when compared with pure buoyancy convection. When water was used as the working fluid, it was reported that no enhancement of heat transfer was observed. Straub repeated the experiments with double-distilled, deionized and tap water, but could not detect any difference in the results. Straub suggested that water contamination could be the reason for the observed behaviour and concluded that further investigation was needed.

Arlabosse et al. [20] performed an experimental analysis of the contribution of Marangoni convection to heat transfer for an air bubble injected in silicon oil. The test cell used in the experiments was an enclosure with a flat heated plate on top, through which an air bubble was introduced, a brass wall at the bottom and plexiglass sidewalls. Based on the results obtained for Prandtl number values of 220, 440 and 880 and Marangoni numbers in the range from 0 to 600, it was determined that the ratio of Marangoni convection heat transfer to heat transfer by pure conduction changed with the square root of the Marangoni number in accordance with $q''_{\mathrm{m}}/q''_{\mathrm{cond}} = 1 + 0.00841Ma^{0.5}$. However, Marangoni con-

vection contribution was relatively small for the configuration and range of parameters investigated.

Another Nusselt number correlation was reported by Betz and Straub [21] who extended the investigations previously performed by Straub et al. [19,22]. For the case where buoyancy and Marangoni flows acted in opposite directions, and the Bond number, the ratio of gravitational and surface tension forces, was equal to 0.1, it was determined from the experiments performed in various liquids that $Nu = 1 + CMa^{0.333}$ where C was dependent on the height of the liquid and the bubble volume.

An interesting observation, obtained during an experimental investigation of boiling heat transfer performed with the very experimental apparatus employed in the present study, was reported by Robinson and Judd [23]. Under conditions of highly subcooled boiling of water, air bubbles which stayed attached to the boiling surface were observed coming out of solution. As a result of the bubble formation, a 20% increase in the heat transfer coefficient was measured. It was postulated that the mechanism responsible for the increased heat transfer rates was Marangoni convection. The conclusion made was in agreement with one made many years earlier by Pike et al. [24], who investigated the effect of dissolved air and carbon dioxide on surface boiling of water and glycerine. The results showed that dissolved gas caused the onset of surface boiling to move to a lower surface temperature for boiling to start, indicating that heat transfer from the surface to the bulk liquid was enhanced. At the time, no explanation was given for the phenomenon observed, but it would seem from the present point of view, that one of the mechanisms involved was Marangoni convection.

3. Experimental investigation

3.1. Boiling vessel

A cross-sectional view of the apparatus used in the experimental study is presented in Fig. 2. The distilled water inside the vessel used as the working fluid was heated by two main heaters located on the outer surface of the vessel. The desired bulk liquid temperature was achieved by simultaneously heating the bulk liquid with the main heaters and cooling it by passing cold water through the subcooling coils within the vessel. The flow rate through the subcooling coils was regulated by a needle valve and monitored continuously. For the bulk liquid temperature measurements, two thermocouples, T_1 and T_2, were inserted into the vessel through fittings in the cover plate and located at approximately 5 and 10 mm from the vessel centerline, ostensibly 40 mm above the working surface.

A copper heater block was mounted in a stainless steel sleeve on the centerline of the stainless steel skirt.

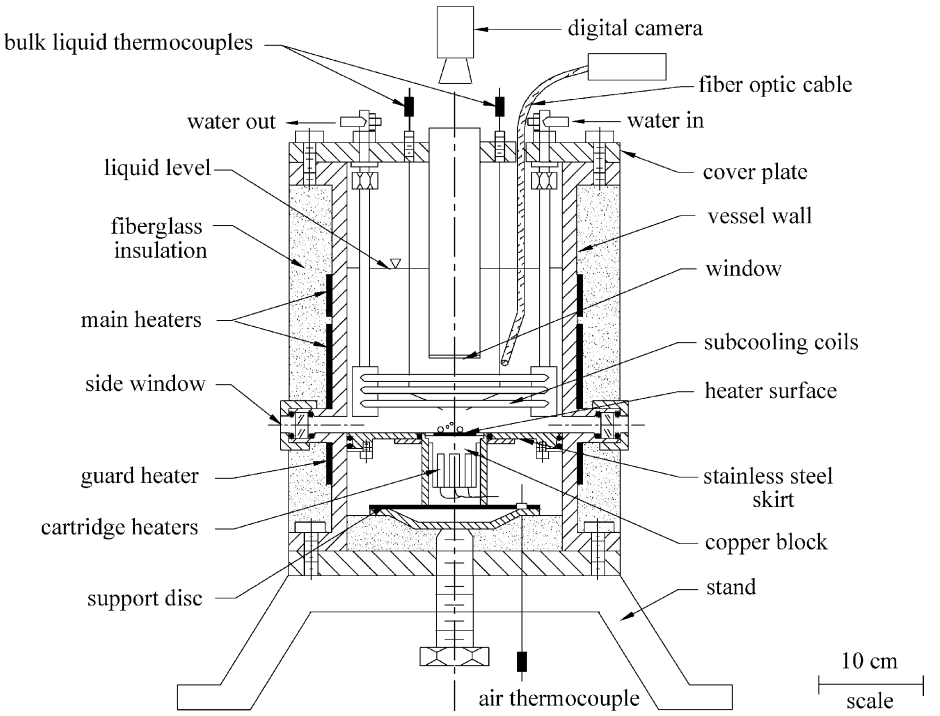

Fig. 2. Experimental set-up.

The skirt was supported by a stainless steel flange welded to the inside of the vessel wall. Two 25 mm diameter circular glass windows were installed at diametrically opposite locations in the outer wall of the vessel affording visual observation of the phenomena occurring at the heater surface.

The temperature of the air between the stainless steel sleeve and the vessel wall was controlled by the guard heater located on the outer surface of the vessel. The presence of the guard heater in this region minimized radial heat losses from the copper block and the axial heat losses from the bulk liquid. The power to the guard heater was varied in such a way that the air temperature around the stainless steel sleeve was as close as possible to the average temperature of the copper block located in the sleeve. In addition, the entire outside surface of the vessel was covered with a fiberglass insulation layer, thereby reducing the heat losses to the environment.

In order to obtain photographic images of bubble formation on the heater surface, a stainless steel tube with a glass window at the bottom was inserted through the cover plate and located approximately 80 mm above the heater surface. The position of the tube was fixed with respect to the cover plate with silicon cement. The glass window was kept clean by a wiper, designed and fixed to the tube for this purpose.

3.2. Heater surface

The heater surface was made from a cylindrical bar of ultra pure copper as shown in Fig. 3. The upper end of the copper block served as the heater surface. The lower end was machined to receive the cartridge heaters that provided the heat flux to the surface. The diameter of the copper block was reduced in order to create an air gap between the block and the surrounding stainless steel sleeve. The air gap served as insulation to minimize the radial heat losses from the copper block. The heater block was welded to the stainless steel sleeve and 10 mm holes were drilled in the copper block to receive the thermocouples T_t, T_m and T_b used for the heat flux determination. In order to reduce the 60 Hz noise around the thermocouples inserted in the copper block, an AC to DC converter was connected in series with the 120 V, 10 A Variac employed to supply power to the cartridge heaters. The circuit was connected to digital multi-

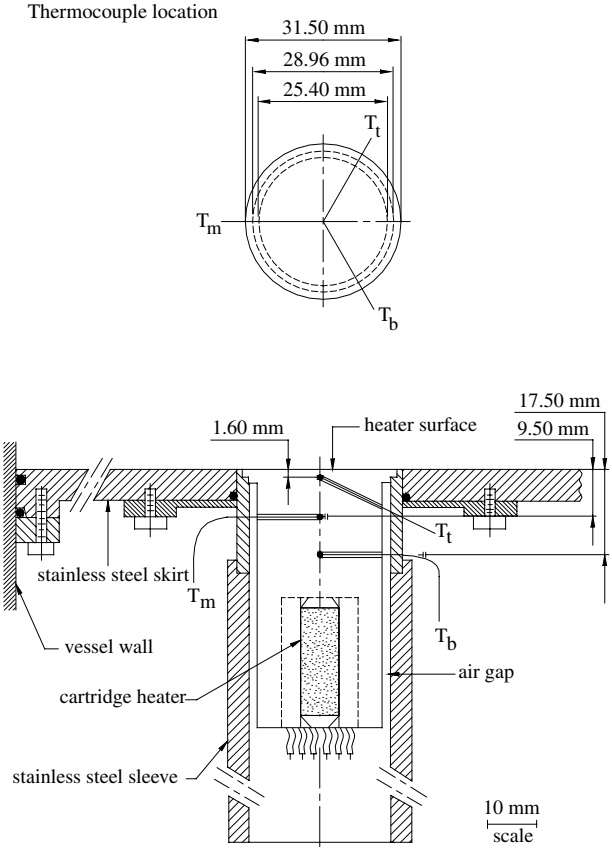

Fig. 3. The heater surface assembly.

meters that provided the current and voltage readings of the power input. Although the electrical power readings were not employed for surface heat flux determination, they were recorded and compared with heat flux values obtained from the axial temperature distribution in the copper block. The agreement provided confidence in the estimation of the radial heat losses present in this region. The average difference was found to be ±4% which was considered to be acceptable.

The heater surface temperature was determined from the measurements of the thermocouples inserted in the copper block which measured the axial temperature distribution. Three thermocouples, T_t, T_m and T_b were inserted into the 10 mm diameter holes drilled into the copper block, located along the copper block centerline at distances of 1.60, 9.50 and 17.50 mm from the heater surface respectively. These temperature measurements were used to determine the heat flux to the heater surface as well.

All thermocouple readings were monitored by the display of an Omega Engineering DP116 Digital Panel Meter. The readings were found to be in a good agreement, ±0.5 °C, with a mercury thermometer and a Fluke 79 (Series III) digital multimeter at the freezing and boiling temperatures of water. Since the thermocouple readings were to be used to determine steady-state conditions, a Phillips PM 8202 single pen chart recorder was employed to indicate the approach of thermal equilibrium. Although the chart recorder was calibrated, it was not used for the thermocouple readings since it was found to be less accurate and less convenient to use than the digital panel meter.

The bulk liquid subcooling level was found in accordance with $\theta_{sub} = T_{sat} - T_\infty$ where T_∞ represents the bulk liquid temperature based on the averaged bulk liquid thermocouple measurements, $T_\infty = \frac{1}{2}(T_1 + T_2)$ and T_{sat} is the water saturation temperature determined from the barometric pressure reading. The uncertainty in the calculated subcooling level is the result of the uncertainty in the bulk liquid temperature measurement which is introduced by the digital panel meter and the thermocouples employed. The meter was calibrated and the maximum error was found to be ±0.5 °C. The resulting uncertainty associated with 40 °C subcooling was found to be 1.25%.

The surface heat flux was calculated by assuming a one-dimensional temperature distribution in the copper block, in accordance with the Fourier law of conduction $q''_c = -k_c\,dT/dz \approx -k_c\,\Delta T/\Delta z$, where k_c represents the thermal conductivity of the copper at the average copper block temperature, and $\Delta T/\Delta z$ is the axial temperature gradient in the copper block, based on the thermocouple measurements T_b, T_m and T_t, obtained at known distances from the surface. Since the ultra pure copper used for the copper block fabrication has high thermal conductivity, it was assumed that the temperature distribution in the copper block was linear so the axial temperature measurements used to determine surface heat flux were fitted with a least squares linear fit. The temperature gradient, $\Delta T/\Delta z$, was determined from the slope of the line obtained and the surface temperature T_w was determined by extrapolation of the line to the surface. The resulting uncertainty in the heat flux measurement was determined to be 4.1%, based on the statistical analysis performed by Shoukri [25] for the distribution of temperature at a hole along the axis of the copper block and further extended by Robinson [26] to the experimental set-up used in the investigation performed.

The surface superheat, θ_{sup}, was determined by $\theta_{sup} = T_w - T_{sat}$ where T_w is the surface temperature and T_{sat} is the water saturation temperature determined by barometric pressure measurement. The uncertainty in the surface temperature measurement and consequently in the value of the surface superheat calculated was estimated to be 1.2%.

3.3. Photographic investigation

In order to obtain clear images of the heater surface needed for the investigation, a Redlake Motion Scope digital camera was placed above the heater surface along the vessel centerline. The use of this camera provided photographs in a digital form which were convenient for analysis. The images were captured by means of a Pentax Macro-Tacumar 1:4/50 lens (Asahi Optical Company) and displayed on a Dell E770s monitor by means of an Intel Pentium III Processor and camera software (Redlake Motion Scope PCI). The necessary illumination of the heater surface was provided by a Fiber Optic Illuminator (Dolan-Jenner Industries, Inc.). The optical fiber cable was admitted to the vessel through an opening in the vessel cover plate. An example of the photographs obtained is shown in Fig. 4.

The photographs obtained clearly displayed the air bubbles attached to the heater surface. The investigation performed required that size and distribution of the air bubbles on the surface be analyzed. For this purpose the "Digitize XY Data" computer program, created by Impera Software, was used. The data was saved as a Microsoft Excel file which was convenient for further calculations.

3.4. Experimental results

In each experiment performed, three different regimes were visually observed, distinguished by the observation of the phenomena occurring at the heater surface. The first regime, identified as natural convection, which was characterized by the absence of bubble activity on the surface and the presence of heat flow currents observed above the heater surface, was present in the initial heat flux range. The second regime, Marangoni

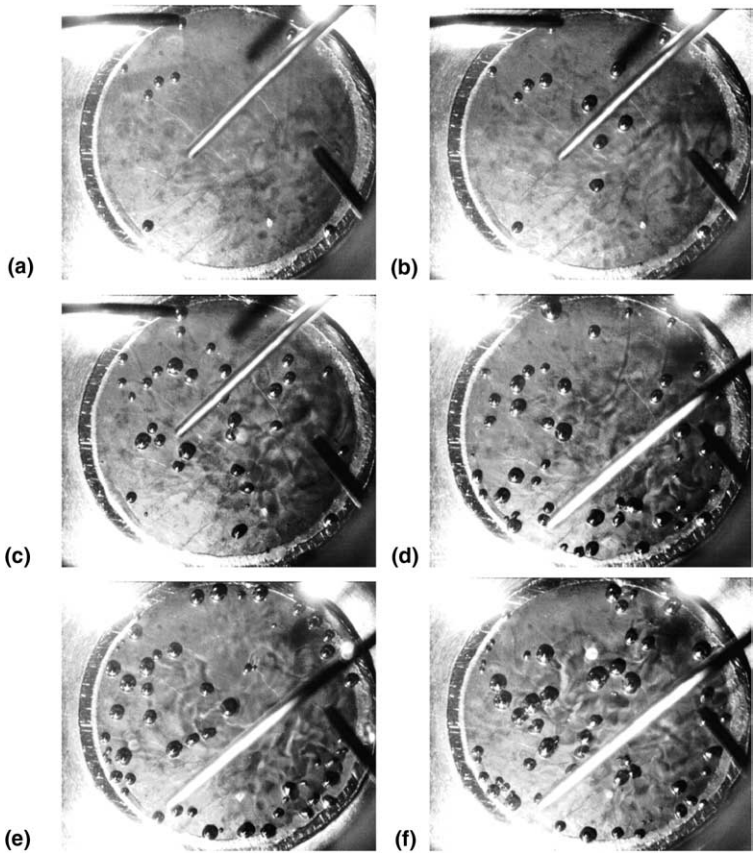

Fig. 4. Air bubble distribution with increasing surface heat flux and 50 °C liquid subcooling: (a) $q'' = 77.2$ kW/m^2, $T_w - T_\infty = 41.8$ °C; (b) $q'' = 93.7$ kW/m^2, $T_w - T_\infty = 45.8$ °C; (c) $q'' = 111.9$ kW/m^2, $T_w - T_\infty = 48.9$ °C; (d) $q'' = 141.2$ kW/m^2, $T_w - T_\infty = 50.4$ °C; (e) $q'' = 164.9$ kW/m^2, $T_w - T_\infty = 56.4$ °C; (f) $q'' = 190.5$ kW/m^2, $T_w - T_\infty = 59.1$ °C.

convection, began when the situation on the surface changed. At certain levels of surface heat flux and liquid subcooling, air bubbles started emerging from the solution and attached themselves to the heater surface. The air bubbles promoted a change in the flow profile in the surrounding bulk liquid, causing a change in the governing heat transfer mechanism. The third regime, nucleate boiling, started when the heat flux reached a value large enough for vapour bubbles to nucleate on the surface. It was characterized by the detachment of the air bubbles, intensive vapour bubble production and a noticeable sound.

The results of the investigation performed are presented in the form of a boiling curve in which the surface heat flux q'' was plotted against the temperature difference between the surface and the bulk liquid temperature, $T_w - T_\infty$, for each of the four subcooling levels investigated. It can be seen in Fig. 5 that for each subcooling level, the three different regimes described earlier are present as indicated by the different trends associated with the different regions of the curves. The change in the boiling curve from natural convection to Marangoni convection was preceded by the appearance of the air bubbles attached to the heater surface. The air bubbles were determined to be spherical by visual observation through the side window of the apparatus. The appearance of the air bubbles did not shift the curve immediately, in as much as it was evident that the change in the governing heat transfer mechanism did not occur until the rate of heat transfer by Marangoni convection exceeded the rate of heat transfer by natural convection.

It was noted that for each value of surface heat flux, the air bubbles would remain at the surface until a maximum size had been attained, after which they would detach and a new bubble would appear at the same spot and pass through the same life cycle. With further increase in surface heat flux, and hence further increase in surface temperature, the number of air bubbles on the surface would increase. This trend continued until the rate of heat transfer by nucleate boiling exceeded the rate of heat transfer by Marangoni convection after which nucleate boiling started at the surface.

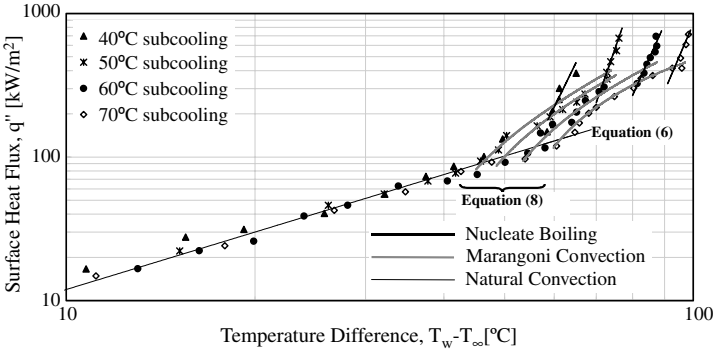

Fig. 5. Boiling curve for various subcooling levels.

4. Analysis and discussion

4.1. Heat transfer model

The analysis is based on a heat transfer model successfully used in the past by Judd and Hwang [27] to analyze boiling heat transfer phenomena. As depicted in Fig. 6, the total heater surface area A_t is considered to be comprised of the total area influenced by the air/vapour bubbles A_{bt} which is associated with Marangoni convection/nucleate boiling heat transfer and the area free of bubbles A_{nc} which is associated with natural convection heat transfer. The total heat transfer rate from the heater surface to the bulk liquid is then given by

$$q''A_t = q''_{nc}A_{nc} + q''_{bt}A_{bt} \tag{2}$$

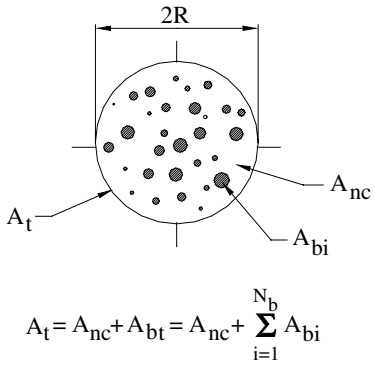

Fig. 6. Representation of the surface heat transfer model.

where q''_{nc} represents the heat flux due to natural convection in the area A_{nc} and q''_{bt} is the heat flux due to Marangoni convection/nucleate boiling in the total area occupied by air/vapour bubbles A_{bt}.

The heat transferred by the bubbles $q''_{bt}A_{bt}$ can be expressed as the product of the heat flux q''_{bt} and the area influenced by bubbles A_{bt} in accordance with

$$q''_{bt}A_{bt} = q''_{bt}\sum_{i=1}^{N_b} A_{bi} \tag{3}$$

where N_b is the total number of bubbles on the surface and A_{bi} is the surface area influenced by a single bubble, taken to be four times the projected bubble area as discussed by Judd and Lavdas [28]. Substituting Eq. (3) into Eq. (2), replacing $A_{nc} = A_t - \sum_{i=1}^{N_b} A_{bi}$ and rearranging yields

$$q'' = q''_{nc} + [q''_b - q''_{nc}]\left(\sum_{i=1}^{N_b} A_{bi}/A_t\right) \tag{4}$$

4.2. Natural convection

Heat transfer between the heated surface and the bulk liquid is attributed to natural convection, the mode of heat transfer resulting from buoyancy effects in which the heat transfer rate due to natural convection is predicted according to Newton's law of cooling by $q_{nc} = \bar{h}A_{nc}(T_w - T_\infty)$.

The average heat transfer coefficient is produced by the flow conditions on the surface which can be expressed in terms of an average Nusselt number $\overline{Nu}_L = \bar{h}L/k_l$. In the case of a circular disk, the characteristic length is $L = A/P = (\pi R^2)/(2\pi R) = R/2$ where R is the radius of the disk. For the present situation, a heated surface facing upward toward a cold liquid, McAdams [29] proposed that

$$\overline{Nu}_L = CRa^{1/4} = C\left\{\frac{g\beta_l(T_w - T_\infty)(R/2)^3}{\nu_l^2}Pr\right\}^{1/4} \tag{5}$$

Khalifa [30] reported that values of the coefficient C could be found in the range from 0.54 to 0.71 in the literature. It was determined that the value of 0.62 gave the best agreement with the experimental data obtained in the present investigation. Substituting the value of the heated surface radius R yields

$$q''_{nc} = 2.126 k_l \left\{ \frac{g\beta}{\nu_l^2} Pr \right\}^{1/4} (T_w - T_\infty)^{5/4} \quad (6)$$

which was used in the evaluation of the surface heat flux rates due to natural convection for comparison with the experimental data where the fluid properties were evaluated at the film temperature $T_{film} = \frac{1}{2}(T_w - T_\infty)$. As seen in Fig. 5, the experimental results obtained fit the curve predicted by Eq. (6) extremely well.

4.3. Incipience of air bubble formation

The change in the governing heat transfer mechanism from natural convection to Marangoni convection was closely related to the appearance of bubbles on the heater surface. A mixture of air and water vapour is present in each bubble and Dalton's law of partial pressures states that the total pressure of the gas mixture is equal to the sum of the partial pressures of its components in accordance with $p_{atmos} = p_{air} + p_{watervapour}$. Air is also present in the bulk liquid, due to its ability to dissolve in water. At equilibrium, the rates of air entering and leaving the liquid, as well as the air partial pressures in the gas and liquid phase, are equal. The equilibrium volume of air dissolved in the bulk liquid is determined by Henry's law. For a dilute solution of air in water, Henry's law states that air is dissolved in the water in the amount proportional to the partial pressure of air above the liquid $p_{air} = Hx$. Raoult's law gives the relationship between the partial pressures of the components in the liquid solution in accordance with $p_{atmos} = Hx + VP(1-x)$. The vapour pressure VP and values of Henry's law constant H corresponding to temperatures in the range 0–100 °C were inserted in the equation above in order to solve for the concentration of air dissolved in a saturated air/water solution x and the variation of air partial pressure p_{air} which is plotted as a function of temperature T in Fig. 7.

The pressure differences indicated in Fig. 7 represent the difference in air partial pressures calculated at the bulk liquid temperature and the surface temperature for the conditions at which the first bubble emerged from the solution at each of the four subcooling levels investigated. According to nucleation theory, small imperfections always present in a heated surface, serve as nucleation cavities for bubble formation. During the initial contact between the surface and the liquid, a mixture of air and water vapour is trapped in the cavities. The partial pressure of the air entrapped in the nucleation cavities decreases as the surface temperature increases. The difference in the partial pressures of the air present in the bulk liquid and the air in the cavity causes air to diffuse from the liquid towards the cavity, resulting in the formation of a bubble. The partial pressure differences are tabulated in Table 1.

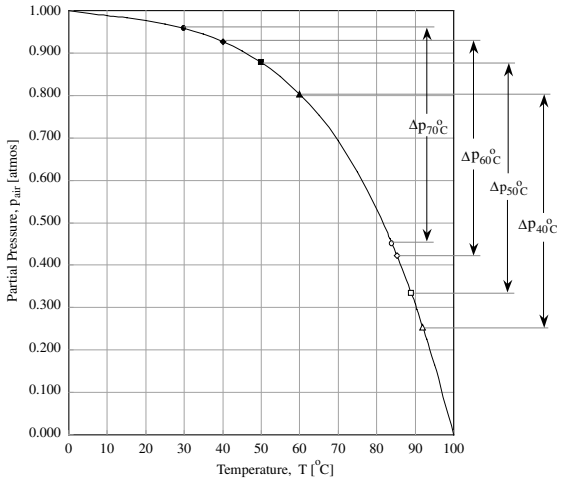

Fig. 7. Analysis of air bubble initiation.

These results were used to estimate the radius of the cavity at which the first air bubble formed in accordance with the relationship $\Delta p = 2\sigma/R_c$. Substitution of the value of the surface tension of water σ and $\Delta p_{average} = 0.533395$ atmos = 54.05 kPa, yields a cavity radius $R_c = 2.3$ μm. Subsequent air bubbles would form at smaller cavities. The value obtained lies in the range of nucleation cavity radii customarily encountered in boiling heat transfer on a pure copper surface.

4.4. Marangoni effect

The air bubbles that emerged from the solution at the nucleation cavities and attached themselves to the heater surface caused a change in the governing heat transfer mechanism from natural convection to Marangoni convection. As depicted in Fig. 8, the bubbles extended the thermal boundary layer at the surface and promoted a flow from the hot wall to the cold bulk liquid due to the surface tension variations along the bubble/liquid interface. Liquid flow near the bubbles is the result of the temperature gradient between the hotter heated surface to which the bubbles were attached and the colder bulk liquid. The temperature difference $\theta_w = T_w - T_\infty$ establishes the flow profile and the heat transfer rates attained.

The heat transfer rate due to Marangoni convection was obtained from Eq. (4), which expresses the heat transfer model introduced earlier. By substituting the expression developed for natural convection heat transfer rates and the values of surface area associated with

Table 1
Analysis of the conditions determining air bubble initiation

θ_{sub} (°C)	T_∞ (°C)	$p_{air\ at\ T_\infty}$ (atmos)	T_w (°C)	$p_{air\ at\ T_w}$ (atmos)	$\Delta p = p_{air\ at\ T_\infty} - p_{air\ at\ T_w}$ (atmos)
40.0	60.0	0.803483	92.0	0.225397	0.578086
50.0	50.0	0.878347	89.0	0.333983	0.544364
60.0	40.0	0.927301	85.3	0.422817	0.504484
70.0	30.0	0.958219	84.0	0.451573	0.506646
					$\Delta p_{average} = 0.533395$

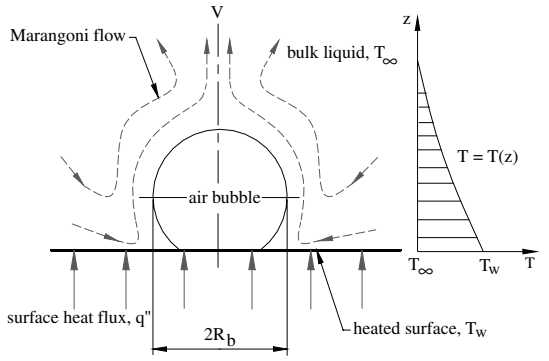

Fig. 8. Marangoni flow around an air bubble.

Marangoni convection and setting $q''_b = q''_m$, the following relationship was obtained

$$\frac{q''_m}{q''_{cond}} = \frac{q''_m}{(T_w - T_\infty)} \frac{L}{k_l} \tag{7}$$

As explained by Arlabosse et al. [20], the reference length should be proportional to the length of the feature over which the flow disturbance extends, so L was set to R_b where R_b is the radius of the bubble.

The values of q''_m/q''_{cond} obtained were plotted against the corresponding Marangoni numbers based upon the same reference length for each combination of the parameters involved and the results obtained are presented in Fig. 9. In order to develop a functional relationship between q''_m/q''_{cond} and Marangoni number to compare with Arlabosse's relationship, the data of the present investigation was fitted with the best parabolic fit. It is seen in Fig. 9 that the relationship obtained fitted the data reasonably well, leading to the conclusion that the problem was modeled correctly. Furthermore, the relationship obtained was identical to that obtained by Arlabosse. It should be mentioned that the experimental set-up afforded a limited range of Marangoni numbers to be investigated such that significant modifications of the experimental assembly would be needed in order to extend the Marangoni number range.

Substitution of Eq. (7) into Eq. (4) leads to

$$\begin{aligned} q'' &= q''_{nc}\left(1 - \sum_{i=1}^{N_b} A_{bi}/A_t\right) + q''_m\left(\sum_{i=1}^{N_b} A_{bi}/A_t\right) \\ &= 2.126 k_l \left\{\frac{g\beta}{\nu_l^2} Pr\right\}^{1/4} (T_w - T_\infty)^{5/4}\left(1 - \sum_{i=1}^{N_b} A_{bi}/A_t\right) \\ &\quad + \frac{k_l}{R_b}(1 + 0.00841 Ma^{1/2})(T_w - T_\infty)\left(\sum_{i=1}^{N_b} A_{bi}/A_t\right) \end{aligned} \tag{8}$$

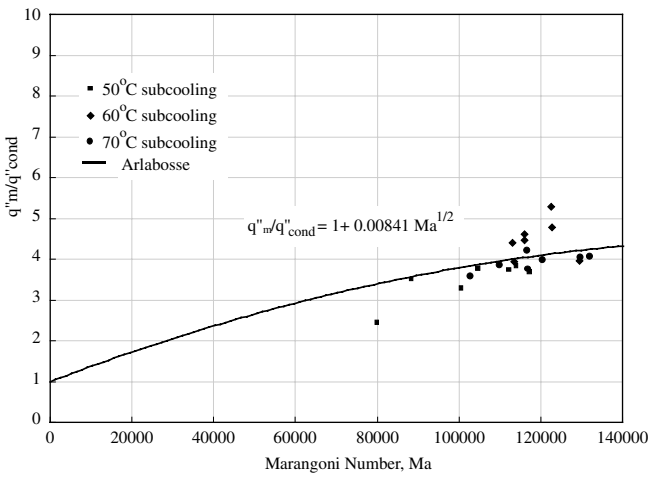

Fig. 9. Variation of the Marangoni convection/conduction heat transfer ratio with Marangoni number.

The total heat transfer rates predicted by Eq. (8) showed good agreement with the experimental data plotted in Fig. 5, leading to the conclusion that the relationship was able to predict the heat transfer rates over a significant range of parameters at different subcooling levels.

4.5. Incipience of nucleate boiling

Transition from the Marangoni convection to the nucleate boiling heat transfer regime occurred when the surface heat flux reached a value large enough for vapour bubbles to nucleate on the surface. Vapour bubbles appeared at the nucleation sites at which air bubble nucleation had occurred during Marangoni convection under the conditions appropriate for nucleate boiling. The change in the heat transfer regime was characterized by rapid air bubble detachment from the heater surface, intensive vapour production and the change in the slope of the curve observed in Fig. 5. The transition from Marangoni convection to nucleate boiling was determined by examining the heat transfer rates.

Classical nucleate boiling heat transfer theories associate the heat transfer rates obtained during nucleate boiling with energy transport from the heater surface to the adjacent superheated liquid layer and its displacement due to the departing vapour bubbles. Han and Griffith [31] postulated that nucleation sites on the surface would have to be surrounded by a superheated liquid layer in order for vapour bubbles to grow. The liquid layer would provide the necessary heat of vapourization, resulting in the vapour bubble growth and eventually departure from the surface. The bubble would remove the portion of the superheated layer contained within its area of influence when departing from the surface and the void created in the thermal boundary layer would be filled by the surrounding colder liquid resulting in a heat flow from the hotter surface to the colder liquid. The time required for the re-establishment of the thermal layer, denoted as the waiting time t_w, is followed by the time during which the bubble grows to departure size, termed the growth time, t_g such that $\tau = t_w + t_g = 1/f$.

Mikic and Rohsenow [32] argued that the instantaneous rate of heat transfer averaged over the whole bubble period τ yields the average heat flux due to nucleate boiling over the area of influence which is given by

$$q''_{nb} = \frac{1}{\tau}\int_0^{\tau}\frac{q(t)}{A}\,dt = f\int_0^{1/f}\frac{q(t)}{A}\,dt = 2\frac{k_l(T_w - T_\infty)}{\sqrt{\pi\alpha_l}}\sqrt{f} = \frac{2}{\sqrt{\pi}}\sqrt{\rho_l C_l k_l}\sqrt{f}(T_w - T_\infty) \quad (9)$$

Evaluation of the properties of water at the saturation temperature 100 °C resulted in the expression

$$q''_{nb} = 1870\sqrt{f}(T_w - T_\infty) \quad (10)$$

The average frequency of bubble emission was obtained from an experimental investigation performed by MacKenzie et al. [33] on the same heater surface employed in the present study which yielded

$$f_0 = 4.53 \times 10^{-3}\theta_{sup}^{3.2} \quad (11)$$

Based on his earlier experimental observations that the bubble emission frequency decreases with increasing subcooling level, Judd [34] has recently proposed a bubble frequency correlation for subcooled boiling conditions expressed by the relationship

$$f/f_0 = \exp(-0.02682\theta_{sub}) \quad (12)$$

The combination of Eqs. (11) and (12) yields

$$f = 4.53 \times 10^{-3}\exp(-0.02682\theta_{sub})\theta_{sup}^{3.2} \quad (13)$$

Expressing the temperature difference in Eq. (10) as $T_w - T_\infty = \theta_{sup} + \theta_{sub}$, the following relationship for nucleate boiling heat flux was obtained

$$q''_{nb} = 125.86\sqrt{\exp(-0.02682\theta_{sub})\theta_{sup}^{3.2}}(\theta_{sup} + \theta_{sub}) \quad (14)$$

Eq. (14) was utilized to compute the heat transfer rates due to nucleate boiling for comparison with the rates attributed to Marangoni convection heat transfer. An expression for the prediction of Marangoni convection heat transfer rates was obtained by combining the previous relationships

$$q''_m = (1 + 0.00841Ma^{1/2})\frac{k_l}{R_b}(T_w - T_\infty) \quad (15)$$

Fig. 10 presents nucleate boiling and Marangoni convection heat fluxes evaluated at the film temperature and an average bubble radius $R_b = 0.55$ mm, based on the photographic investigation performed. It is seen in Fig. 10 that there are two regions distinguished by the dominant heat transfer mechanisms. The four separate curves on the graph for each subcooling level investigated represent the Marangoni convection dominant region. In this zone, Marangoni convection heat transfer rates are initially greater than the corresponding nucleate boiling heat transfer rates, indicating that although the wall temperature was higher than the saturation temperature, boiling was suppressed by the Marangoni convection heat transfer mechanism. Only after the nucleate boiling heat transfer rates became greater than the Marangoni convection heat transfer rates did vapour bubbles begin to form on the surface and boiling started.

Experimental observations confirmed the conclusion expressed above. For the four subcooling levels investigated, the transition from Marangoni convection to nucleate boiling regime occurred when nucleate boiling heat transfer rates exceeded the corresponding Marangoni convection heat transfer rates. The intersections of the curves plotted in Fig. 10 for subcooling levels of

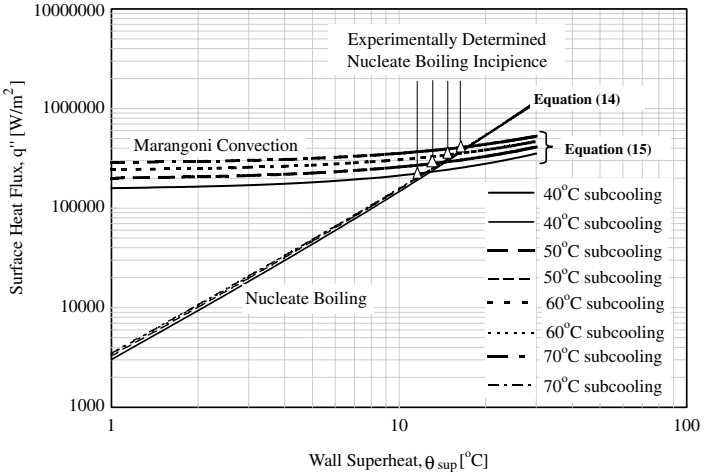

Fig. 10. Incipience of nucleate boiling.

40, 50, 60 and 70 °C, indicate that nucleate boiling starts at superheats of 13, 15, 16 and 18 °C respectively. The nucleate boiling incipience superheats reported in Petrovic [35] confirm these values.

5. Conclusions

An experimental investigation was performed in order to examine the contribution of Marangoni convection to the rate of heat transfer in subcooled nucleate pool boiling using distilled water heated on a copper heater surface at atmospheric pressure and subcooling levels of 40, 50, 60 and 70 °C. For each subcooling level investigated, heat flux to the heater surface was gradually increased from zero to a value large enough for nucleate boiling to become fully developed. During the experimental investigation, the natural convection phenomenon was confirmed and a relationship present in the literature was found to give excellent agreement with the experimental data obtained.

With increasing surface heat flux, a change from natural convection to Marangoni convection heat transfer was observed. Analysis of the data obtained provided confirmation of the presence of the Marangoni convection phenomenon. The ratio of the Marangoni convection heat flux and the heat flux due to pure conduction was found to be in perfect agreement with the relationship previously reported by Arlabosse. The heat transfer rates predicted by the theory developed were found to give excellent agreement with the experimental data, supporting the conclusion that the situation encountered during the experimental investigation was indeed Marangoni convection.

With further increase in the surface heat flux, a change from Marangoni convection to nucleate boiling heat transfer was observed. The correlations developed confirmed the nucleate boiling phenomenon and demonstrated that the change from Marangoni convection to nucleate boiling heat transfer occurred when the heat transfer rates associated with nucleate boiling exceeded those associated with Marangoni convection.

References

[1] J. Straub, The role of surface tension for two-phase heat and mass transfer in the absence of gravity, Exp. Thermal Fluid Sci. 9 (1994) 253–273.
[2] R.A. Pearson, On convection cells induced by surface tension, J. Fluid Mech. 4 (1958) 489–500.
[3] L.E. Scriven, C.V. Sternling, On cellular convection driven by surface-tension gradients: effects of mean surface tension and surface viscosity, J. Fluid Mech. 19 (1964) 321–352.
[4] K.A. Smith, On convective instability induced by surface-tension gradients, J. Fluid Mech. 24 (1966) 401–414.
[5] N.O. Young, J.S. Goldstein, M.J. Block, The motion of bubbles in a vertical temperature gradient, J. Fluid Mech. 6 (1959) 350–356.
[6] J.L. McGrew, F.L. Bamford, T.R. Rehm, Marangoni flow: an additional mechanism in boiling heat transfer, Science 153 (1966) 1106–1107.
[7] B.K. Larkin, Thermocapillary flow around a hemispherical bubble, AIChEJ 16 (1970) 101–107.
[8] E.S. Gaddis, The effect of liquid motion induced by phase change and thermocapillarity on the thermal equilibrium of a vapour bubble, Int. J. Heat Mass Transfer 15 (1972) 2241–2250.
[9] Y.S. Kao, D.B.R. Kenning, Thermocapillary flow near a hemispherical bubble on a heated wall, J. Fluid Mech. 53 (1972) 715–735.
[10] V. Hupik, G.D. Raithby, Surface-tension effects in boiling from a downward-facing surface, J. Heat Transfer 94 (1972) 403–409.

[11] D. Schwabe, J. Metzger, Coupling and separation of buoyant and thermocapillary convection, J. Cryst. Growth 97 (1989) 23–33.
[12] K. Wozniak, G. Wozniak, T. Rosgen, Particle–image–velocimetry applied to thermocapillary convection, Exp. Fluids 10 (1990) 12–16.
[13] G. Wozniak, K. Wozniak, H. Bergelt, On the influence of buoyancy on the surface tension driven flow around a bubble on a heated wall, Exp. Fluids 21 (1996) 181–186.
[14] H. Ben Hadid, B. Roux, Buoyancy and thermocapillary driven flows in differentially heated cavities for low-Prandtl-number fluids, J. Fluid Mech. 235 (1992) 1–36.
[15] D. Raake, J. Siekmann, Temperature and velocity fields due to surface tension driven flow, Exp. Fluids 7 (1989) 164–172.
[16] C.H. Chun, D. Raake, G. Hansmann, Oscillating convection modes in the surroundings of an air bubble under a horizontal heated wall, Exp. Fluids 11 (1991) 359–367.
[17] M. Kassemi, N. Rashidnia, Steady and oscillatory thermocapillary convection generated by a bubble, Phys. Fluids 12 (2000) 3133–3146.
[18] C. Reynard, R. Santini, L. Tadrist, Experimental study of the gravity influence on the periodic thermocapillary convection around a bubble, Exp. Fluids 31 (2001) 440–446.
[19] J. Straub, M. Zell, B. Vogel, What we learn from boiling in microgravity, Microgravity Sci. Technol. 6 (1993) 239–247.
[20] P. Arlabosse, L. Tadrist, H. Tadrist, J. Pantaloni, Experimental analysis of the heat transfer induced by thermocapillary convection around a bubble, J. Heat Transfer 122 (2000) 66–73.
[21] J. Betz, J. Straub, Numerical and experimental study of the heat transfer and fluid flow by thermocapillary convection around gas bubbles, Heat Mass Transfer 37 (2001) 215–227.
[22] J. Straub, J. Betz, R. Marek, Enhancement of heat transfer by thermocapillary convection around bubbles—a numerical study, Numer. Heat Transfer 25 (1994) 501–518.
[23] T. Robinson, R.L. Judd, Heat transfer enhancement due to Marangoni convection around gas bubbles attached to a heated surface, in: Proceedings of the 17th Canadian Congress of Applied Mechanics, Hamilton, Canada, May 30–June 3, 1999, pp. 259–260.
[24] F.P. Pike, P.D. Miller, K.O. Beatty, Effect of gas evolution on surface boiling at wire coils, Chemical Engineering Progress—Symposium Series, vol. 51, 1955, pp. 13–19.
[25] M.S.M. Shoukri, Nucleation Site Activation in Saturated Boiling, M.Eng. Thesis, McMaster University, Canada, 1974.
[26] A.J. Robinson, A Study of the Effect of Subcooling on Bubble Formation in Nucleate Pool Boiling, M.Eng. Thesis, McMaster University, Canada, 1997.
[27] R.L. Judd, K.S. Hwang, A comprehensive model for nucleate pool boiling heat transfer including microlayer evaporation, J. Heat Transfer 98 (1976) 623–629.
[28] R.L. Judd, C.H. Lavdas, The nature of nucleation site interaction, J. Heat Transfer 102 (1980) 461–464.
[29] W.H. McAdams, Heat Transmission, third ed., McGraw-Hill, New York, 1954 (Chapter 7).
[30] A.J.N. Khalifa, Natural convection heat transfer coefficient—a review; I. Isolated vertical and horizontal surfaces, Energy Conver. Manage. 42 (2001) 491–504.
[31] C. Han, P. Griffith, The mechanism of heat transfer in nucleate pool boiling, Int. J. Heat Mass Transfer 8 (1965) 887–904.
[32] B.B. Mikic, W.M. Rohsenow, A new correlation of pool-boiling data including the effect of heating surface characteristics, J. Heat Transfer 91 (1969) 245–250.
[33] H. MacKenzie, R.L. Judd, M.S.M. Shoukri, Experiments in narrow gap convective boiling, in: Proceedings of the 17th Canadian Congress of Applied Mechanics, Hamilton, Canada, May 30–June 3, 1999, pp. 269–270.
[34] R.L. Judd, Influence of Acceleration on Subcooled Nucleate Boiling, Ph.D. Thesis, University of Michigan, USA, 1968.
[35] S. Petrovic, Marangoni Heat Transfer in Subcooled Nucleate Pool Boiling, M.A.Sc. Thesis, McMaster University, Hamilton, Ontario, Canada, 2003.